UNDER REVIEW

RESCIENCE C

Replication / Computational Neuroscience

[Re] Cortical network effects of subthalamic deep brain stimulation in a thalamo-cortical microcircuit model

Celine Soeiro[1, ID] **and Antonio C. Roque**[2, ID]

[1]Universidade de São Paulo, FFCLRP, Departamento de Computação e Matemática, Ribeirão Preto, Brazil – [2]University of Sao Paulo, FFCLRP, Department of Physics, Ribeirao Preto, Brazil

Edited by
(Editor)

Reviewed by
(Reviewer 1)
(Reviewer 2)

Received
–

Published
–

DOI
–

Abstract Parkinson's disease is a degenerative disorder of the central nervous system associated to motor and nonmotor symptoms. Local field potential recordings reveal an elevated power in the beta band ($\sim 13 - 30$ Hz) as a key indicator of altered cortical activity in parkinsonism. Deep brain stimulation of the subthalamic nucleus has been successfully used in the treatment of Parkinson's disease by suppressing pathological activity in the beta band and alleviating motor symptoms. A possible mechanism to explain the efficacy of deep brain stimulation of the subthalamic nucleus is the antidromic activation of pyramidal neurons in the primary motor cortex. The firing of these neurons would have a modulatory effect on the activity of the thalamo-cortical loop, reducing power in the beta band. Recently, Farokhniaee and Lowery proposed a model of the thalamo-cortical microcircuit that simulates this mechanism. The Farokhniaee and Lowery model was implemented in Matlab, and the goal of this work is to reimplement it in Python and reproduce a selection of its results.
A replication of farokhniaee2021cortical.

1 Introduction

Parkinson's disease (PD) is a degenerative disorder of the central nervous system that predominantly affects dopamine-producing neurons in the substantia nigra (SN), one of the basal ganglia nuclei [1]. The pathophysiological changes associated with the death of dopaminergic neurons critically impact the functioning of neurons in the primary motor cortex (M1), which are related to the command and execution of movements, thereby causing PD [2, 3].

One of the primary indicators of altered cortical activity in PD is an exaggerated increase of power in the beta band oscillations ($\sim 13-30$ Hz), as measured in local field potential (LFP) recordings from deep cortical layers in rats [4] and electrocorticography recordings in awake rats [5] and PD patients [6, 7]. Studies in animal models demonstrate that excessive oscillatory activity in the beta band is not confined solely to M1 but extends throughout the entire cortico-basal-thalamo-cortical loop [5, 8, 9].

Deep Brain Stimulation (DBS) has been successfully employed in PD treatment, suppressing pathological activity in the beta band and alleviating motor symptoms [10, 11]. In DBS treatment, high-frequency electrical stimuli (> 80 Hz) are applied via chronically implanted electrodes in regions of the basal ganglia (subthalamic nucleus, STN, and internal globus pallidus, GPi) or the thalamus [12, 13]. However, despite its clinical efficacy, the mechanisms of action of DBS are not yet well understood, and one reason for this is the difficulty in simultaneously recording the activity of multiple neurons in the involved brain structures.

Correspondence should be addressed to Celine Soeiro (celinesoeiro@gmail.com)
The authors have declared that no competing interests exists.
Code is available at https://github.com/celinesoeiro/TCM-Model.

Computational modeling emerges as a tool capable of aiding in the understanding of the mechanisms responsible for the effects of DBS. Various types of computational models of the complete or partial cortico-basal ganglia-thalamic-cortical circuit have been used to contribute to elucidating these mechanisms [14, 15, 16, 17, 18, 19, 20, 21].

In particular, Farokhniaee and Lowery [21] have recently proposed a model that allows the analysis of the effects of DBS on the thalamo-cortical circuit under conditions similar to those present in PD. The model explores the so-called hyperdirect pathway from deep pyramidal neurons in M1 to STN [22]. It is known from experimental studies that chronically implanted electrodes that deliver electrical pulses to STN also stimulate, via the hyperdirect pathway, axons of deep M1 pyramidal neurons. This "antidromic" stimulation induces firing in the deep M1 pyramidal neurons, which modulates cortical excitability and reduces beta oscillations [10, 23, 24].

The model of Farokhniaee and Lowery, which will be referred here as FL model, was originally implemented in Matlab and the code in available on ModelDB (https://modeldb.science/266941). Our objective in this work was to reimplement the FL model in Python and reproduce its main result, namely, the attenuation of the exaggerated beta rhythm by direct injected currents to deep M1 pyramidal neurons. All codes used in this reimplementation are available in the GitHub of the first author (https://github.com/celinesoeiro/TCM-Model/).

2 Methods

The microcircuit model consists of six different structures, four in M1, the supragranular or surface (S) layer, the granular or middle (M) layer, the infragranular or deep (D) layer, and the cortical interneurons (CI), and two in the thalamus, the thalamic reticular nucleus (TR) and the thalamo-cortical relay nucleus (TC). Neurons of the S, M, S and TC structures are excitatory, and neurons of the CI and TR structures are inhibitory (Figure 1).

The M1 structures contain subpopulations of different neuron types. Neurons are described by the Izhikevich model [25, 26] (see section 2.1) with parameters adjusted to display different intrinsic firing patterns: regular spiking (RS) and intrinsically bursting (IB) in the case of excitatory neurons, and fast spiking (FS) and low threshold spiking (LTS) in the case of inhibitory neurons. The model contains 540 neurons distributed by the different structures as shown in Table 1.

Structure	Neuron type					
	RS	IB	FS	LTS	TC	TR
S (100 neurons)	50%	50%	-	-	-	-
M (100 neurons)	100%	-	-	-	-	-
P (100 neurons)	70%	30%	-	-	-	-
IC (100 neurons)	-	-	50%	50%	-	-
TC (100 neurons)	-	-	-	-	100%	-
TR (100 neurons)	-	-	-	-	-	100%

Table 1. Distribution of neuron types by the different structures of the FL model

2.1 Neuron model

For each neuron i in structure j, where $i = 1, \cdots, N_j$ (N_j being the number of neurons in structure j) and $j = 1, 2, 3, 4, 5, 6$, corresponding, respectively, to structures S, M, D, CI,

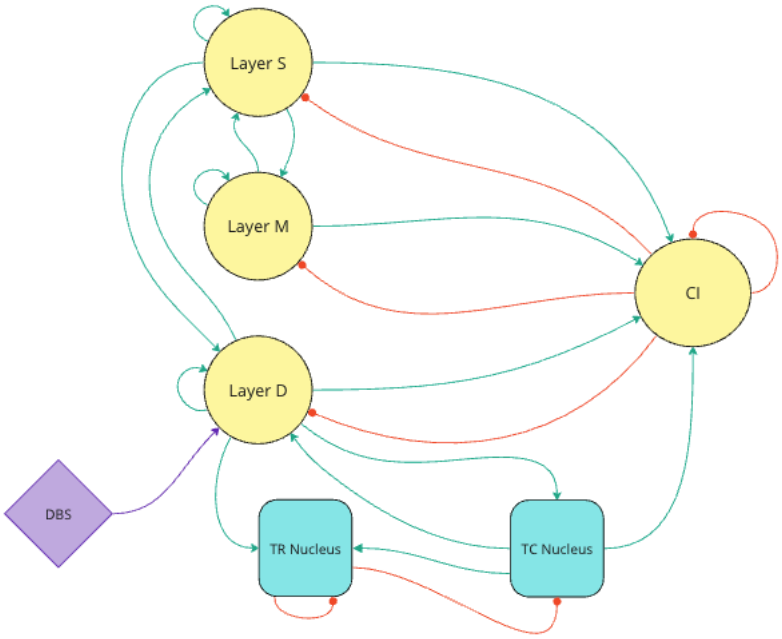

Figure 1. Scheme of the FL model. Yellow circles represent the M1 structures (S, M, D and CI) and cyan rounded squares represent the thalamic structures (TR and TC). The lilac diamond represents the STN DBS through the hyperdirect pathway. Excitatory and inhibitory connections are represented by cyan and red lines, respectively. The DBS input to layer D is excitatory.

TR and TC, its dynamics is given by the coupled differential equations of the Izhikevich model [25, 26], (Equations 1 and 2),

$$\begin{cases} \dot{v}_{ij} &= 0.04v_{ij}^2 + 5v_{ij} + 140 - u_{ij} + I_{ij,\mathrm{dc}} + \xi(t) + I_{ij,\mathrm{syn}} + I_{j,\mathrm{bkg}} + I_{\mathrm{dbs}}\delta_{j3} \\ \dot{u}_{ij} &= a_{ij}(b_{ij}v_{ij} - u_{ij}), \end{cases} \tag{1}$$

$$\text{if} \quad v_{ij} \geq v_{pij} + \zeta(t), \quad \text{then} \quad \begin{cases} v_{ij} \leftarrow c_{ij} \\ u_{ij} \leftarrow u_{ij} + d_{ij}. \end{cases} \tag{2}$$

In these equations, v_{ij} is the membrane voltage and u_{ij} is the membrane recovery variable. The parameters a_{ij}, b_{ij}, c_{ij} and d_{ij} determine the firing pattern of the neuron. The Izhikevich model is dimensionless, but the scales of the variables v_{ij} and t were adjusted to correspond to physical values in mV and ms, respectively. When the membrane voltage reaches the threshold value v_{pij}, a spike is assumed to occur and both v_{ij} and u_{ij} are instantaneously updated as shown in (2).

The injected current terms in (1) are the following: $I_{ij,\mathrm{dc}}$ is an external direct current (DC) with value adjusted to bias the neuron i in structure j so that it is just above firing threshold; $\xi(t)$ is a Gaussian white noise term [27] scaled so that the mean firing rates of the neurons are compatible with experimental recordings; $I_{ij,\mathrm{syn}}$ represents the synaptic currents, described by the Tsodyks-Markram model [28, 29] (see section 2.2); $I_{j,\mathrm{bkg}}$ is a structure-dependent background input noise given by Poissonian spike-trains with fixed rates $\nu_j = (20 + 2\epsilon_j)$ Hz $(j = 1, \cdots, 6)$, where ϵ_j is randomly drawn from a Gaussian distribution of zero-mean and unit variance; and $I_{\mathrm{dbs}}\delta_{j3}$ represents the DBS current applied only to neurons of structure D $(j = 3)$, where δ_{jk} is the Kronecker delta function.

Finally, $\zeta(t)$ is another Gaussian white noise term added to the threshold potential of neuron i in structure j. The scale of this threshold noise was set to one third of the scale of $\xi(t)$.

The set of values for the parameters of the Izhikevich neurons given by FL model are identical of those given in the original article given by Izhikevich [25]. However the DC current values given in the FL model Supplementary Material and the ones displayed in their provided code are different, after some tests we decided to use the DC current values from the provided code because they display a better response than the ones provided in the text. The neuron parameters can be found in Table 2.

	a	b	c	d	I_{dc}	v_p
RS	0.02	0.2	−65	8	3.5	30
IB	0.02	0.2	−55	4	3.6	30
FS	0.1	0.2	−65	2	3.8	30
LTS	0.02	0.25	−65	2	0.6	30
TC	0.02	0.25	−65	0.05	0.5	30
TR	0.02	0.25	−65	2.05	0.6	30

Table 2. Parameters of the Izhikevich neurons

To introduce heterogeneity among neuron models, so that different neurons from each of the six classes have different dynamics, the FL model adopted the same strategy of Izhikevich [25]: for the excitatory neurons (RS, IB, and TC), indexed by i, $(a_i, b_i) = (a, b)$ and $(c_i, d_i) = (c, d) + (15, -6)r_i^2$, where r is a uniformly distributed random variable between 0 and 1, and a, b, c, and d are the values in Table 2 for each of these types of excitatory neurons, respectively. Similarly, for the inhibitory neurons (FS, LTS, and TR), their parameters are given by $(a, b) + (0.08, -0.05)r_i$ and $(c_i, d_i) = (c, d)$, where a, b, c, and d correspond to the parameters for these neurons in Table 2.

2.2 Synapse model

The synaptic model utilized to implement connections between neurons in the FL model is the Tsodyks-Markram (TM) model [28, 29] The TM model is a phenomenological model that describes both short-term synaptic depression and facilitation. Given the presynaptic spike time t_{ps}, it determines the postsynaptic current (PSC), I_{syn}, by the coupled differential equations,

$$\begin{cases} \dot{x} = \frac{-x}{\tau_f} + U(1 - x^-)\delta(t - t_{\mathrm{ps}} - \Delta) \\ \dot{R} = \frac{(1-R)}{\tau_d} - x^+ R^- \delta(t - t_{\mathrm{ps}} - \Delta) \\ \dot{I}_{\mathrm{syn}} = \frac{-I_s}{\tau_s} + A u^+ R^- \delta(t - t_{\mathrm{ps}} - \Delta), \end{cases} \tag{3}$$

where R is a normalized variable ($0 < R < 1$) representing the fraction of neurotransmitters (termed "synaptic resources") that remain available for use after synaptic transmission; x represents the fraction of synaptic resources immediately available for use (the probability of neurotransmitter release at a given moment); U is the increment in x produced by the arrival of a spike at the pre-synaptic terminal; A is the amplitude of the synaptic response that would be produced if all neurotransmitters were released (absolute synaptic response); Δ takes into account the synaptic and axonal transmission delay; τ_f, τ_d and τ_s are the time constants of the variables x, R and $_{\mathrm{syn}}$, respectively; and δ is the Dirac delta function. In these equations, x^- and R^- represent the values of these variables just before the arrival of a spike, and x^+ indicates the value of x just after a spike.

The interaction between the dynamics of x and R determines whether the combined effect of the two results in a transient facilitation, depression, or no change in the amplitude of the PSC over the course of a stimulus train. Synapses that display these three types of short-term dynamics are called facilitating (F), depressing (D) and pseudo-linear (P) [30]. The FL model used the parameters given by Markram et al. [30] to implement F, D and P synapses (Table 3).

Excitatory synapses					
	τ_f	τ_d	τ_s	U	A
Facilitating	670	138	3	0,09	0.20
Depressing	17	671	3	0,5	0.63
Pseudo-linear	326	329	3	0,29	0.17
Inhibitory synapses					
Facilitating	376	45	11	0,016	0.08
Depressing	21	706	11	0,25	0.75
Pseudo-linear	62	144	11	0,32	0.17

Table 3. Values of synaptic parameters

The parameter A has a sum equal to 1 for both excitatory and inhibitory synapses. This means that 20% of the amplitude of the excitatory postsynaptic potential (EPSP) is due to facilitating synapses, 63% is due to depressing synapses, and 17% is due to pseudo-linear synapses; and 8% of the amplitude of the inhibitory postsynaptic potential (IPSP) is due to facilitating synapses, 75% is due to depressing synapses, and 17% is due to pseudo-linear synapses.

2.3 Thalamo-cortical microcircuit model

The basic topology of the FL thalamo-cortical microcircuit model consists of a fully connected network with random connections between neurons. Given two structures X and Y (which can be the same) composed of N_X and N_Y neurons, respectively, the strengths of the connections from X to Y are determined by an $N_X \times N_Y$ matrix of uniformly distributed random numbers in the range $[0, 1]$, multiplied by a factor W_{XY} that determines the maximum strength of connections. The values of synaptic strengths were adjusted to produce a simulated LFP in cortical layer D that resembles the LFP recorded under normal conditions. Subsequently, Farokhniaee and Lowery [21] adjusted the synaptic strengths to implemented a new connectivity matrix that generates a LFP signal in layer D with high power in the beta band, representing a parkinsonian condition.

We reimplemented this procedure in Python and generated the two connection matrices shown in Figure 2. The matrix on the left implements a normal condition, and the matrix in the right implements a parkinsonian condition.

Comparing the matrix on the right in Figure 2 with the one in Figure S1 of the suplementary material of the original article, it can be observed that they are consistent. From the normal state to the parkinsonian state, there is an increase in synaptic coupling from TC to D and CI, from M to S, and from TR to TC; and there is a decrease in synaptic coupling from CI to D, from S to M, from D to both TC and TR, and from TC to TR.

Using the connection matrix it is possible to simulate both the normal and the parkinsonian conditions just by switching the connection weights from one structure to another. In our code the connection matrix is in the *tcm_params* file under the name *coupling_matrix_normal*, which holds the values for the normal condition, and *coupling_matrix_PD*, which holds the value for the parkinsonian condition.

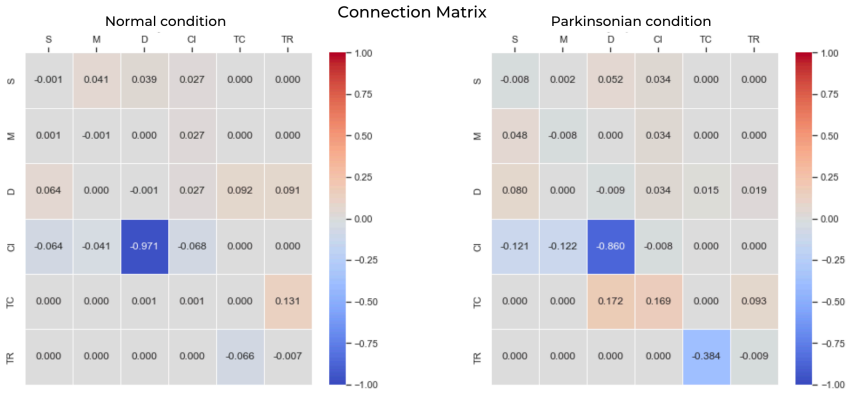

Figure 2. Mean normalized synaptic coupling weights (from rows to columns) within and between different structures of the reimplemented FL model. The left matrix represents the normal condition and the right matrix represents the parkinsonian condition.

All model structures can be found in the github repository as functions: *S_nucleus*, responsible to model the S layer, can be found in the file *S_nucleus_noise*, *M_nucleus*, responsible to model the M layer, can be found in the file *M_nucleus_noise*, *D_nucleus*, responsible to model the D layer, can be found in the file *D_nucleus_noise*, *CI_nucleus*, responsible to model the CI layer, can be found in the file *CI_nucleus_noise*, *TC_nucleus*, responsible to model the TC nucleus, can be found in the file *TC_nucleus_noise* and *TR_nucleus*, responsible to model the TR nucleus, can be found in the file *TR_nucleus_noise*.

2.4 Stimulation protocol

The DBS current I_{dbs} consists of a train of Dirac pulses with frequency f_{dbs} and amplitude A applied to 25% of neurons in D during a certain time. We used a stimulation protocol like the one in the original article. The model under parkinsonian conditions was simulated for a time T, which was divided in three equal parts. From $t = 0$ to $t = T/3$ and from $t = 2T/3$ to $t = T$, the parkinsonian model was simulated without DBS input (DBS off), and from $t = T/3$ to $t = 2T/3$ the model was simulated with DBS input (DBS on). In all (*in silico*) experiments done, only the DBS frequency f_{dbs} varied. The pulse amplitude remained constant at $A = 335$ as in the original article. We used three f_{dbs} values: 80 Hz, 130 Hz and 180 Hz. The simulation time was $T = 15$ s.
The network activity was characterized by simulating the LFP recorded from layer D. The layer D LFP was simulated by summing EPSCs generated by layer D neurons and IPSCs to layer D neurons from CI layer neurons using the equation,

$$LFP(t) = \frac{1}{4\pi\sigma r}\left(\sum_{i=1}^{n_D} EPSC_i(t) + \sum_{i=1}^{n_{CI}} IPSC_i(t)\right), \tag{4}$$

where $\sigma = 0.27$ S/m is the electric conductivity of the extracellular medium and $r = 100$ µm is the mean distance between the recording electrode and the neurons.

After obtaining the LFP signal, it was filtered using a third-order Butterworth bandpass filter to select the signal in the beta band (13-30 Hz), which is the frequency range of interest for this study. The filter was implemented using the *butter* function imported from the SciPy package. The power spectral density (PSD) of the LFP was estimated using the Welch method, implemented by the *welch* function from the SciPy package.

The main goals were to observe the effect of high-frequency DBS on the power of beta rhythm in the parkinsonian condition, and to study whether increasing the DBS fre-

quency would decrease the beta power.

To accomplish this task it was necessary to create a function capable of receiving a frequency and compare the parkinsonian state before and after the DBS stimulus. This function was named *dbs* and is under the file *dbs_compare*. The goal of this function is to compare the results of DBSs in different frequencies. To see how the DBS affects the system in only one frequency use the file *DBS* and switch the *dbs_freq* parameter under the file *tcm_params*.

3 Implementation details

Following the best practices of programming, the model parameters were put in a separeted file. This file includes the time parameters, neurons, synapses, noise and DBS parameters, and the connection matrices, both to simulate the normal and the parkinsonian conditions.

3.1 Neuron model

The implementation of the Izhikevich model in the first author's GitHub was created in two ways. The first was used to implement the model as given in the original article by Izhikevich [25]. The goal with this first implemetation was to obtain a Python model of the neuron in order to use it in the FL model. In order to achieve this, a folder was created, named *Izhikevich_neuron*, and inside this folder, the user will find a file named *izhikevich_neuron_simulations*, which runs the file *izhikevich_neuron* simulating all neurons in the Izhikevich article [25]. Comparing the obtained results with the results in the original article, it was possible to see that the neuron model was perfoming as expected.

The second implementation is used in the FL model. It contains functions for v and for u, which can be found in the file *model_functions* under the names *izhikevich_dvdt* and *izhikevich_dudt*, respectively. These functions are called by the functions that run each structure to compute the next values of the neurons' membrane voltages and recovery variables.

3.2 Synapse model

Following similar steps as the ones for the neuron model, the synapse model was also modeled in two ways. The first with the intention of ensuring that the model is correct (found inside the *tm_synapses* folder), and the second thinking about the FL model implementation (found inside the *model_functions* file).
In the first implementation, the TM model was based on 4 functions that can be found inside the *tm_synapses* folder, in the file *model_functions*, one that simulates an excitatory synapse dominated by depression (*tm_syn_excit_dep*), one that simulates an excitatory synapse dominated by facilitation (*tm_syn_excit_fac*), another one that simulates an inhibitory synapse dominated by depression (*tm_syn_inib_dep*), and another function that simulates an inhibitory synapse dominated by facilitation (*tm_syn_inib_fac*). Those functions were called for each neuron type in the FL model, each in a different file under the *tm_synapses* folder. These files are named *TM_syn_RS*, *TM_syn_IB*, *TM_syn_FS*, *TM_syn_LTS*, *TM_syn_TC* and *TM_syn_TR* for neurons RS, IB, FS, LTS, TC and TR, respectively.
The second implementation combined facilitation, depression and pseudo-linear synapses in one function, following the implementation in the original article, and is on the file *model_functions*, under root as *tm_synapse_eq*. This function was used in each model

structure to get the PSC. The same approach was used to create the function *tm_synapse_poisson_eq*, which was used to create the synaptic activity generated by the background Poissonian spike trains. Finally, they were also combined in the function *I_dbs*, which creates the DBS synaptic current injected on neurons from structure D.

3.3 The TCM model

The approach to implement this model was to split and conquer, meaning that the full model was divided into smaller pieces, each containing a part of the cortex until the full model was obtained.
The firts step can be found in file *step-1-cortical*, which contains the cortex modeled with only the D layer and the CI. The thalamus was modeled by a spike generator modeled by a Poisson process. The second step (*step-2-cortical* file) added layer S to the cortical model, and the third step (*step-3-cortical* file) added layer M. The fourth step was to model the thalamus, which is in file *step-4-tc-normal*, simulating the normal condition, and *step-4-tc-PD*, simulating the parkinsonian condition. The DBS treatment was simulated in file *DBS*.
In summary, to simulate the model under normal brain conditions the user should run the file *step-4-tc-normal*, and to simulated the model under parkinsonian conditions the user should run the file *step-4-tc-PD*. To simulate the DBS treatment, the user should go the *tcm_params* file, search for the variable *dbs_freq* and set this variable to the desired frequency in Hz. After that, the user should run the file *DBS*.
For signal analysis there are two files: *dbs_compare*, which holds a function called *dbs* that receives a value of frequency that is the desired DBS frequency value. This file returns a comparison of the 3 DBS frequencies used in this article, 80Hz, 130Hz and 180Hz. The second file is called *signal_analysis*, which has 3 functions: *normal_condition*, simulating the network in normal conditions (same as the one found in *step-4-tc-normal* file); *PD_condition*, simulating the network in parkinsonian condition (same as the one found in *step-4-tc-PD* file); and *dbs*, simulating the network under parkinsonian condition with DBS stimulus (same as the one found in *DBS* file). The goal of this file is to compare all the recorded activities in the network and compare their power spectral densities (PSDs).

4 Results

The first goal of this work was to replicate the FL model in Python and to simulate both normal and parkinsonian conditions. This was achieved and the raster plot simulating the parkinsonian condition is shown in Figure 3. The simulation ran for a period of 15 seconds, as in the simulation in Figure 3(a) of the original article [21]. Both raster plots display an elevated activity of the cortical interneurons, specially of the FS neurons, and a high level of syncronization among neurons in layer D, especially of RS neurons.
Figure
Figure 4 shows a comparison of the PSDs of the simulated LFPs for both the normal and the parkinsonian conditions. In the normal condition, the power is well distributed within the 15-25 Hz range and decays for higher frequencies, but in the parkinsonian condition there is a strong peak within the high beta range ($\sim$ 25-30 Hz).
The second goal was to simulate a high-frequency DBS application to neurons in layer D under parkinsonian conditions and verify if this would reduce the excess power in the beta band, as in the original article. The DBS frequency used in the original article was 130 Hz, and, for comparison with the original article, the simulated LFP in our replication for this DBS frequency is shown in Figure 5. Although the tracings are not identical (note that the original article does not provide the scale of the vertical axis), the replication result is consistent with that of the original article. The simulated DBS application significantly reduced oscillatory activity in the beta band during the application period.

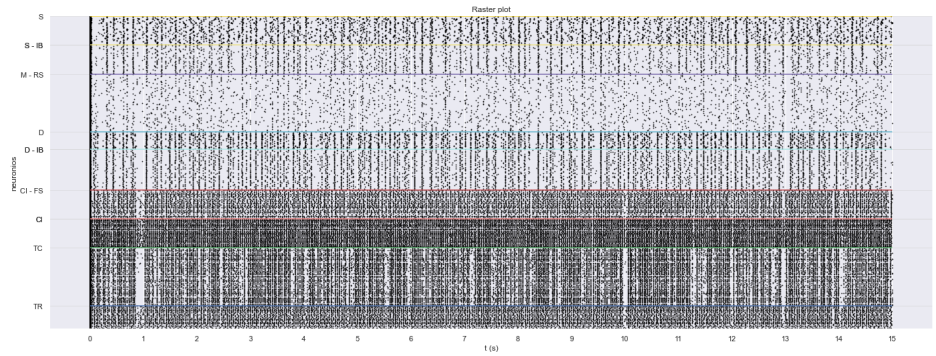

Figure 3. Raster plot of the reimplemented thalamocortical model simulating the parkinsonian condition under 15 seconds of simulation.

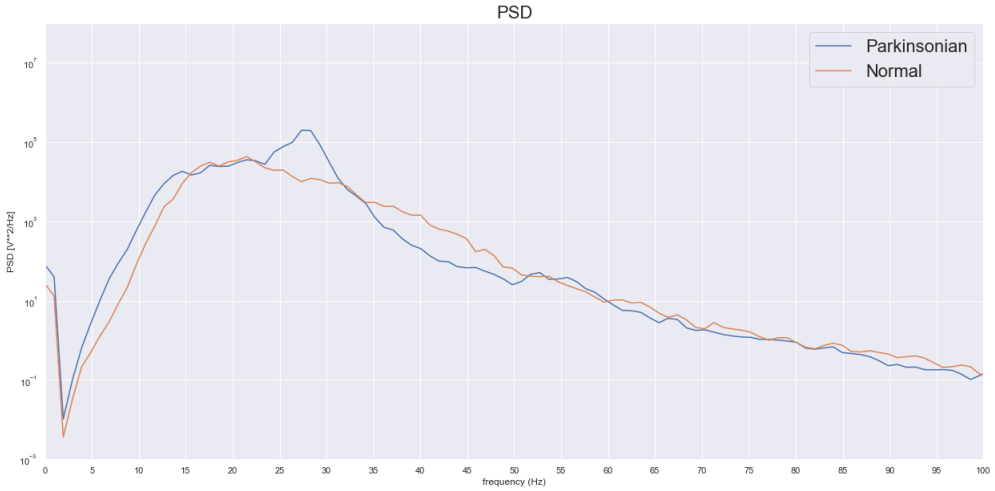

Figure 4. Power spectral density of the simulated LFP under normal (orange trace) and parkinsonian (blue trace) conditions.

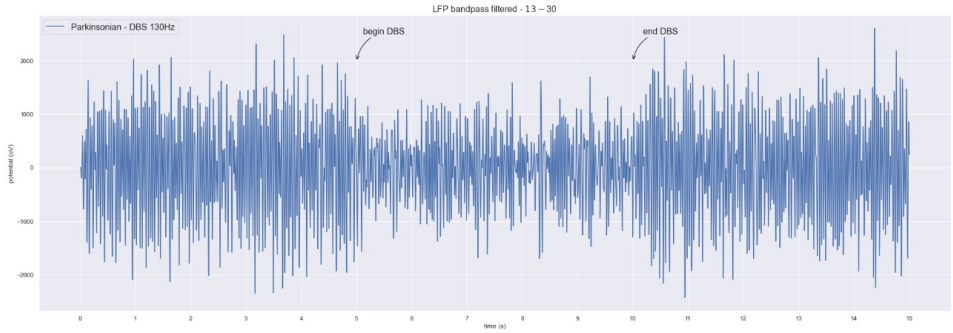

Figure 5. LFP from layer D filtered for the beta band in the parkinsonian condition with DBS stimulation at 130 Hz applied between seconds 5 to 10 in a 15 seconds simulation.

In our replication, we conducted a study on the effect of two other DBS frequencies on the LFP under parkinsonian conditions, 80 Hz and 180 Hz. The effects of these two DBS frequencies, as well as the one at 130 Hz, on the PSD of the LFP are shown in Figure 6. The 80 Hz DBS causes a slight reduction in power in the beta band, the 130 Hz DBS produces a much greater reduction, and the 180 Hz DBS produces a reduction comparable to that of 130 Hz. This suggests that there is not a very significant gain, in terms of

reduction in beta power, when increasing the DBS frequency from 130 to 180 Hz.

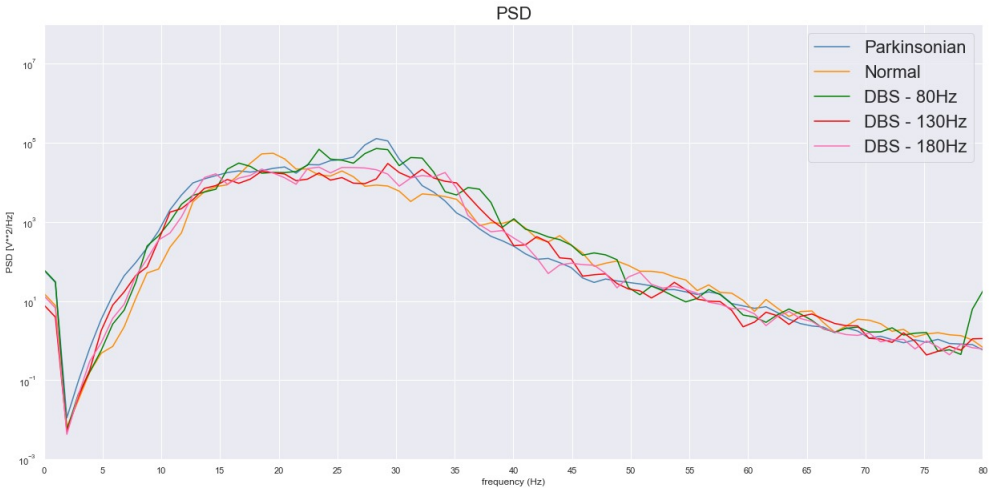

Figure 6. PSD of the simulated LFP from layer D for normal (orange), parkinsonian condition without DBS (blue), parkinsonian conditions with DBS at 80 Hz (green), parkinsonian conditions with DBS at 130 Hz (red), and parkinsonian conditions with DBS at 180 Hz (pink). The PSDs for the parkinsonian conditions without and with DBS were estimated for the simulation intervals $0 < t < 5$ s and $5 < t < 10$, respectively.

5 Discussion

In our DBS simulation of DBS, it was shown that the 80 Hz frequency already produces some reduction in power in the beta band, but this reduction is more effective when the frequency is increased to 130 Hz. An even higher increase in frequency to 180 Hz did not produce a significant reduction in power compared to the reduction achieved at 130 Hz, suggesting that there may be a plateau of possible frequencies in terms of efficiency in reducing beta power. Given the limited values of frequencies used in this study, it can only be concluded that this plateau includes frequencies of 130 Hz and 180 Hz, but it is not possible to say if it starts below or extends beyond this frequency range.
From a clinical perspective, there is a commonly used frequency range for DBS treatments, ranging from 60 Hz to 200 Hz [31]. However, there is no consensus on the effectiveness of increasing the stimulation frequency. Some authors mention that the higher the stimulation frequency, the greater the decrease in power in the beta band [32], while others note that the reduction in pathological behavior is not very significant at frequencies above 130 Hz [33].

6 Conclusion

We were able to reimplement the FL model in Python and replicate its main result, at least qualitatively. Our results support the central concept of the original article, namely that antidromic activation of the hyperdirect pathway during STN DBS affects cortical neuronal activity and results in a range of phenomena, including alteration of neural firing rates and reduction of beta activity.

7 Acknowledgments

ACR is supported by the São Paulo Research Foundation (FAPESP) grant 2013/07699-0 (CEPID NeuroMat) and by the Brazilian National Council for Scientific and Technological Development (CNPq) Research Productivity Grant 303359/2022-6.

References

1. M. J. Armstrong and M. S. Okun. "Diagnosis and treatment of Parkinson disease: a review." In: **Journal of the American Medical Association** 323 (2020), pp. 548–560.
2. G. W. Arbuthnott and M. Garcia-Munoz. "Are the symptoms of Parkinsonism cortical in origin?" In: **Computational and Structural Biotechnology Journal** 15 (2016), pp. 21–25.
3. R. Savica, B. F. Boeve, and M. M. Mielke. "When do -synucleinopathies start? An epidemiological timeline: a review." In: **Journal of the American Medical Association Neurology** 75 (2018), pp. 503–509.
4. Q. Li, Y. Ke, D. C. W. Chan, Z. M. Qian, K. K. L. Yung, H. Ko, G. Arbuthnott, and W. H. Yung. "Therapeutic deep brain stimulation in Parkinsonian rats directly influences motor cortex." In: **Neuron** 76 (2012), pp. 1030–1041.
5. A. Sharott, P. J. Magill, D. Harnack, A. Kupsch, W. Meissner, and P. Brown. "Dopamine depletion increases the power and coherence of -oscillations in the cerebral cortex and subthalamic nucleus of the awake rat." In: **European Journal of Neuroscience** 21 (2005), pp. 1413–1422.
6. C. De Hemptinne, N. C. Swann, J. L. Ostrem, E. S. Ryapolova-Webb, M. San Luciano, N. B. Galifianakis, and P. A. Starr. "Therapeutic deep brain stimulation reduces cortical phase-amplitude coupling in Parkinson's disease." In: **Nature Neuroscience** 18 (2015), pp. 779–786.
7. D. Whitmer, C. De Solages, B. Hill, H. Yu, J. M. Henderson, and H. Bronte-Stewart. "High frequency deep brain stimulation attenuates subthalamic and cortical rhythms in Parkinson's disease." In: **Frontiers in Human Neuroscience** 6 (2012), pp. 1–18.
8. C. Hammond, H. Bergman, and P. Brown. "Pathological synchronization in Parkinson's disease: networks, models and treatments." In: **Trends in Neuroscience** 30 (2007), pp. 357–364.
9. Y. Tachibana, H. Iwamuro, H. Kita, M. Takada, and A. Nambu. "Subthalamo-pallidal interactions underlying parkinsonian neuronal oscillations in the primate basal ganglia." In: **European Journal of Neuroscience** 34 (2011), pp. 1470–1484.
10. S. Li, G. W. Arbuthnott, M. J. Jutras, J. A. Goldberg, and D. Jaeger. "Resonant antidromic cortical circuit activation as a consequence of high-frequency subthalamic deep-brain stimulation." In: **Journal of Neurophysiology** 98 (2007), pp. 3525–3537.
11. E. Moro, A. M. Lozano, P. Pollak, Y. Agid, S. Rehncrona, and J. Volkmann. "Long-term results of a multicenter study on subthalamic and pallidal stimulation in Parkinson's disease." In: **Movement Disorders** 25 (2010), pp. 578–586.
12. M. C. Rodriguez-Oroz et al. "Bilateral deep brain stimulation in Parkinson's disease: a multicentre study with 4 years follow-up." In: **Brain** 128 (2005), pp. 2240–2249.
13. R. G. Cury, V. Fraix, A. Castrioto, M. A. Pérez Fernández, P. Krack, S. Chabardes, E. Seigneuret, E. J. L. Alho, A. L. Benabid, and E. Moro. "Thalamic deep brain stimulation for tremor in Parkinson disease, essential tremor, and dystonia." In: **Neurology** 89 (2017), pp. 1416–1423.
14. C. C. McIntyre, W. M. Grill, D. L. Sherman, and N. V. Thakor. "Cellular effects of deep brain stimulation: model-based analysis of activation and inhibition." In: **Journal of Neurophysiology** 91 (2004), p. 14571469.
15. J. Rubin and D. Terman. "Stimulation of the subthalamic nucleus eliminates pathological thalamic rhythmicity in a computational model." In: **Journal of Computational Neuroscience** 16 (2004), pp. 211–235.
16. M. D. Johnson and C. C. McIntyre. "Quantifying the neural elements activated and inhibited by globus pallidus deep brain stimulation." In: **Journal of Neurophysiology** 100 (2008), pp. 2549–2563.
17. G. Kang and M. M. Lowery. "Interaction of oscillations, and their suppression via deep brain stimulation, in a model of the cortico-basal ganglia network." In: **IEEE Transactions on Neural Systems and Rehabilitation Engineering** 21 (2013), pp. 244–253.
18. A. Mandali, M. Rengaswamy, V. S. Chakravarthy, and A. A. Moustafa. "A spiking Basal Ganglia model of synchrony, exploration and decision making." In: **Frontiers in Neuroscience** 9 (2015), p. 191.
19. K. Kumaravelu, D. T. Brocker, and W. M. Grill. "A biophysical model of the cortex-basal ganglia-thalamus network in the 6-OHDA lesioned rat model of Parkinson's disease." In: **Journal of Computational Neuroscience** 40 (2016), pp. 207–229.

20. E. J. Müller and P. A. Robinson. "Quantitative theory of deep brain stimulation of the subthalamic nucleus for the suppression of pathological rhythms in Parkinson disease." In: **PLoS Computational Biology** 14 (2018), e1006217.
21. A. Farokhniaee and M. M. Lowery. "Cortical network effects of subthalamic deep brain stimulation in a thalamo-cortical microcircuit model." In: **Journal of Neural Engineering** 18.5 (2021), p. 056006.
22. D. Milardi et al. "The cortico-basal ganglia-cerebellar network: past, present and future perspectives." In: **Frontiers in Systems Neuroscience** 13 (2019), p. 61.
23. C. Dejean, B. Hyland, and A. G. "Cortical effects of subthalamic stimulation correlate with behavioral recovery from dopamine antagonist induced akinesia." In: **Cerebral Cortex** 19 (2009), pp. 1055–1063.
24. R. Kuriakose et al. "The nature and time course of cortical activation following subthalamic stimulation in Parkinson's disease." In: **Cerebral Cortex** 20 (2010), pp. 1926–1936.
25. E. M. Izhikevich. "Simple model of spiking neurons." In: **IEEE Transactions on neural networks** 14.6 (2003), pp. 1569–1572.
26. E. M. Izhikevich. **Dynamical Systems in Neuroscience: The Geometry of Excitability and Bursting**. Cambridge, Massachussetts, EUA: The MIT Press, 2007.
27. W. Gerstner, W. M. Kistler, R. Naud, and L. Paninski. **Neuronal Dynamics: From Single Neurons to Networks and Models of Cognition**. Cambridge, Reino Unido: Cambridge University Press, 2014.
28. M. Tsodyks and H. Markram. "The neural code between neocortical pyramidal neurons depends on neurotransmitter release probability." In: **Proceedings of the National Academy of Sciences (USA)** 94 (1997), pp. 719–723.
29. M. Tsodyks, K. Pawelzik, and H. Markram. "Neural networks with dynamic synapses." In: **Neural computation** 10.4 (1998), pp. 821–835.
30. H. Markram et al. "Reconstruction and simulation of neocortical microcircuitry." In: **Cell** 163 (2015), pp. 456–492.
31. J. Waldthaler, A. Sperlich, A. König, C. Stüssel, F. Bremmer, L. Timmermann, and D. Pedrosa. "High (130 Hz)- and mid (60 Hz)-frequency deep brain stimulation in the subthalamic nucleus differentially modulate response inhibition: A preliminary combined EEG and eye tracking study." In: **NeuroImage: Clinical** 37 (2023), p. 103314.
32. F. Su, K. Kumaravelu, J. Wang, and W. M. Grill. "Model-based evaluation of closed-loop deep brain stimulation controller to adapt to dynamic changes in reference signal." In: **Frontiers in neuroscience** 13 (2019), p. 956.
33. J. Volkmann. "Deep brain stimulation for the treatment of Parkinson's disease." In: **Journal of clinical neurophysiology** 21.1 (2004), pp. 6–17.